

HENRYK MARCAK\*

### SEISMICITY IN MINES DUE TO ROOF LAYER BENDING

### ROZWÓJ SEJSMICZNOŚCI GÓRNICZEJ W REZULTACIE UGINANIA SIĘ STROPU

The experience, which has been obtained in Polish mining allow us to conclude that the bending of the roof layer over an exploited seam is one of the most important factors influencing the risk of strong seismic emissions. The seismic consequences of plastic deformations during roof layer bending are discussed in the paper. The linear distribution of seismic shock epicentres and trends in the development of seismic energy and event frequency, are expected before very strong seismic events that greatly increase rock-burst risk.

The proposed model of inelastic deformations allow us to correlate the seismic data and results of mining observations, such as convergence of the roof layer and the changes of wells diameter drilled in the roof layer in assessing the risk of rock-bursting.

**Keywords:** mining, seismic events, bending, generation model, rock-bursts

Doświadczenia uzyskane w polskim górnictwie wskazują na to, że uginanie warstw stropowych nad eksploatowanym pokładem jest jednym z najważniejszych czynników, które zwiększają ryzyko wystąpienia silnej emisji sejsmicznej w kopalniach podziemnych. W artykule przedstawiono rozważania dotyczące związku pomiędzy sejsmicznością a rozwojem deformacji plastycznej w uginającej się warstwie stropowej. Jedną z konsekwencji tej deformacji jest liniowy rozkład epicentrow wstrząsów i istnienie trendów wzrostowych w rozwoju energii sejsmicznej i trendów spadkowych w rozwoju częstości pojawiania się wstrząsów w okresie poprzedzającym bardzo silną relaksację energii sejsmicznej. Taka relaksacja jest bezpośrednio związana z ryzykiem powstania tąpnięcia.

Zaproponowany w artykule model deformacji niesprężystej pozwala korelować dane sejsmiczne z wynikami obserwacji górniczych, takich jak konwergencja stropu czy zmiana średnicy otworów wierconych w stropie eksploatowanego pokładu, które zgodnie z dotychczasowym doświadczeniem są związane z ryzykiem powstania tąpnięcia.

**Słowa kluczowe:** górnictwo, zjawisko sejsmiczne, uginanie warstwy, modele generacyjne, tąpnięcia

\* AGH UNIVERSITY OF SCIENCE AND TECHNOLOGY, AL. MICKIEWICZA 30, 30-059 KRAKOW, POLAND;  
E-mail: [marcak@agh.edu.pl](mailto:marcak@agh.edu.pl)

## 1. Introduction

There are two mining regions in Poland subject to rock-burst risk; one is the coal basin in Upper Silesia, and the second, the copper region in Lower Silesia. Special procedures have been introduced to make the exploitation in the rock-burst prone mines safer. An exploitation system has been designed specifically to avoid a concentration of stresses, and those measures continuously, the subsidence ratio and properties of rocks under stress. Seismological measuring systems have been installed in many Polish mines, which record seismic waves throughout the mines. On the basis of the recorded signals, the location of a seismic event hypocenter and its energy are estimated. Seismic catalogues containing times of seismic events occurrences, the coordinates of events hypocenters and their energies are prepared continuously by mining geophysical staff.

There are many publications related to seismic emissions in Polish underground mines. The subjects of those papers are studies of the structure of seismic events before a rock burst. There are also papers, in which the generation of seismic emission is considered (Lasocki, 2005, 2008; Marcak, 2002; Dubiński & Konopko, 2000; Dubiński, 1999).

Two approaches can be distinguished in the works related to development of seismic emissions before strong seismic event occurrence. In one, the advanced statistical methods are used for the extraction of information from the empirical data. For example, Hurst rescaled range analysis and the autocorrelation function have been used to show that the seismic interevent time and interevent distance have a long and short memory, thereby increasing the chance of strong seismic events predictions (Węglarczyk & Lasocki, 2009).

In the second approach, the “a priori model” is introduced in order to enrich the empirical information. For example in the publication (Orlecka-Sikora, 2010), the physical mechanism of interactions between the mining induced seismic events is discussed. The transfer of Coulomb stress is assumed to influence the generation of mining induced seismicity. This assumption has been verified statistically using a catalogue of seismic events that occurred in the “Rudna” mine in the Legnica-Głogow Copper District in Poland.

In the present paper and in the papers (Marcak, 2011a, 2011b) the second approach is represented.

In both mining regions in Poland, in Upper Silesia and in Lower Silesia, strong sedimentary layers appear in the roof of exploited parts of the rock masses. They consist of sandstone in the coalmine basin and limestone and dolomite in the copper mining areas. The bending of these layers is the result of exploitation and in Poland is treated as one of the most important factors behind the build up of stresses, which result in the strong rock bursts. Controlling the ratio of the roof layer bending is a method to control the stress in the surroundings of the exploited area.

Usually elastic deformations are considered in mining models. In this paper, the plastic deformation due to stresses resulting in roof layer bending is analyzed. The chosen seismic data from the “Rudna” mine in the Legnica-Głogow Copper District in Poland has been used to ascertain the relationship between the developments of the inelastic deformation of the roof layer and the increase of seismic events energy. In this paper the seismic consequences of the stress development resulting from bending beams are discussed.

## 2. Roof layer bending

In general, the stress involved into body by bending depends on its shape.

Bending can be symmetrical, if the cross-section of the homogeneous element subject to bending is symmetrical, or asymmetrical, if the cross-section of the homogeneous element subject to bending is also asymmetrical. For an unhomogeneous medium the centroid axes represented by the lines joining the centroid of each cross-section along the length of an axial line, is not neutral.

When the rock beam is stressed by transverse loading force, the amount of bending deflection and the curvature of bending depends on the value of force and the beam's material properties. The stretched and compressed sides of the beam are opposite when the curvature is changed from positive into negative. (Fig. 1). Two stresses are important in analyzing the appearance of mining shocks, normal and shear.

For the rectangular rod of length  $L$  and cross-section  $s$  the normal stress caused by bending

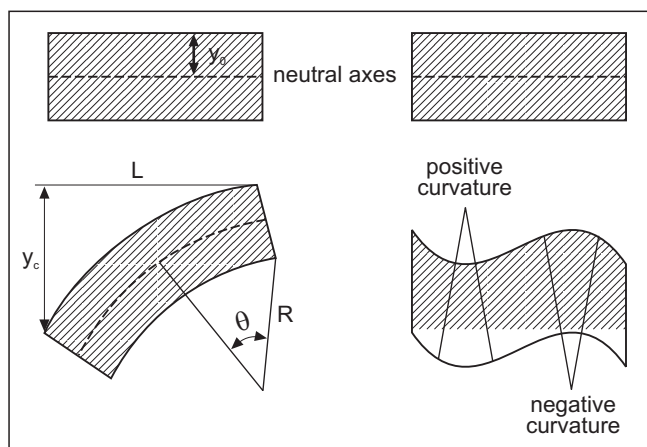


Fig. 1. The beam bending,  $R$  – the curvature of the beam.  $L$  – Distance from the fixed point of beam

$\sigma_{xx}$  can be described by the following formula (Boresi et al., 1993):

$$\sigma_{xx} = \frac{M}{I} (y - y_0) = \frac{E}{R} (y - y_0) \quad I = \frac{sL^3}{12} \quad (1)$$

and shear stresses

$$\tau = \frac{VQ}{It} \quad (2)$$

where  $M$  is the bending moment ( $W \cdot L$ ),  $E$  represents the modulus of elasticity,  $I$  is the moment of inertia,  $W$  is the load,  $L$  is the length of road,  $y - y_0$  is the distance to the neutral axes,  $R$  is the radius of curvature of the beam,  $V$  is the shear force,  $Q$  – the first moment of area  $A_s$  about the

$z$  axis passing through the centroid,  $A_s$  is the area between the free surface and the line at which the shear stress is being calculated and  $t$  represents the thickness perpendicular to the centerline.

Normal stress  $\sigma_{xx}$  in bending increase linearly with  $y - y_0$  while shear stress has maximum on the neutral axes. The maximum of normal stresses runs along the maximum bending curvature line while the shear stresses there are equal to zero and intensify with the increasing distance from this line.

The basic equation is obtained in the form (Boresi et al., 1993):

$$\frac{d^2 y_0}{dx^2} = \frac{M}{EI} \quad (3)$$

The bending force  $q(x)$  is then expressed with the formula

$$q(x) = EI \frac{d^4 y_0}{dx^4} \quad (4)$$

and shear force  $V(x)$  by

$$V(x) = EI \frac{d^3 y_0}{dx^3} \quad (5)$$

If the equations are extended into the bending plane, the straight line of maximum bending force is created hereinafter called 'lineament'.

Budryk (Saustowicz, 1965) obtained the solution to equation (1) for conditions, which appear in the underground mines. If  $p$  is the vertical stress component in the upper border of the horizontal bending layer, then the solution has the form:

$$y_0 = \frac{p}{c} + e^{-\beta x} \frac{pL}{4\beta^2 EI} (-L \sin(\beta x) + (1 + \frac{2}{\beta}) \cos(\beta x)) \quad (6)$$

and the vertical stress  $\sigma_{zz}$  in the seam can be written as:

$$\sigma_{zz} = p - \beta^2 p L e^{-\beta x} (-L \sin(\beta x) + (1 + \frac{2}{\beta}) \cos(\beta x)) \quad (7)$$

Where

$$\beta = \sqrt[4]{\frac{c}{4EI}} \quad (8)$$

$c$  — the elastic compliance.

This equation is used in Poland for estimation of the stress distribution in the roof surrounding the exploited ore. Bending deflection can be controlled with appropriate mining techniques and the exploitation by the room and pillar method allow one to designing the ratio of roof layer deflection.

In this paper the inelastic deformations in the bending roof layer and its connection with seismic emissions in underground mines are considered.

There are only two possible modes of rock fracturing: namely, ductile and brittle. In general, the main difference between a brittle and ductile fracturing can be attributed to the amount of plastic deformations that the material undergoes before fracture occurs. Ductile materials demonstrate large amounts of plastic deformation whereas brittle materials show little or no plastic deformation before fracture. In this paper the ductile deformation of the bending roof layer is discussed, and is the result of normal bending stresses. However, the plastic deformations in the external parts of the roof layer can trigger brittle horizontal splitting along sub-layers border and it can be treated as a source of seismic energy.

Plastic deformation during the roof layer bending phase develops in a specific way.

As the bending loading momentum is gradually increased the greatest stresses occur at the outermost parts of the roof layer. As shown in Fig. 2 the plastic (ductile) deformation starts from the outer parts of the roof layer, whilst the inner section is still elastic. An increase of bending momentum causes a migration of plastic regions into the central part of the layer, causes redistribution of the local stresses surrounding the ductile zone (Marcak, 2002) (shear force appearing along the zone) and in the final stage it turns into a fracture. Due to a decrease of the normal stresses the fractured part also breaks off along the horizontal border with the next part. Such fracturing in outer parts of the layer is randomly repeated along the line of maximum bending (lineament). When the density of fractured sections in the margin part of roof layer is large enough they then coalesce, the moment of the bending resistance drops and the fracture develops inwards in the layer. Due to penetration of the ductile fracture the process of brittle fracturing along the deeper horizontal border is repeated and associated seismic event with one or two orders higher appears. This hierarchic process can be repeated again. In the end the bending turns asymmetrical and the inertia moment has the form of a tensor which has, in a two-dimensional case, three independent elements:

$$I_x = \int y^2 ds \quad I_y = \int x^2 ds \quad I_{xy} = \int xy ds \quad (9)$$

Deeper penetration of the ductile zone causes the intensive disturbances of horizontal shear force distribution and larger deformations of the structure of the layer.

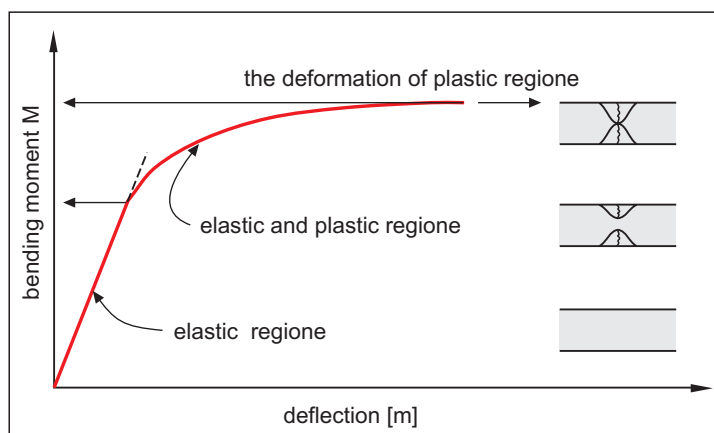


Fig. 2. Plastic deformation during bending of the roof layer

### 3. Seismic response of the bending stresses

As a result of ductile deformations just before the seismic event, the stage called “hardening” is reached, (Rice & Ruina; 1983; Rice, 1980) meaning that the shear stress level increases very rapidly with only a slight deformation. In practical terms the hardening stops deformations, and in particular the bending deflection. After obtaining maximum shearing value, in the second stage of deformation known as “softening”, the very intensive deformation and intensive deflation of the roof layer is associated with seismic energy release. Both stages can be observed as the changes in the convergence intensity (the tighten of exploitation area) shown in fig. 3. A decrease and intensive increase in roof subsidence is observed before and after shocks.

The effect of the seismic energy release (Kayama, 1997) can be described with the use of the seismic moment  $M$  where:

$$M = \mu \bar{u} \Sigma \tag{10}$$

where

- $\mu$  — module of rigidity,
- $\Sigma$  — the area of rupture on which seismic energy is realized,
- $\bar{u}$  — the average displacement on the  $\Sigma$  surface.

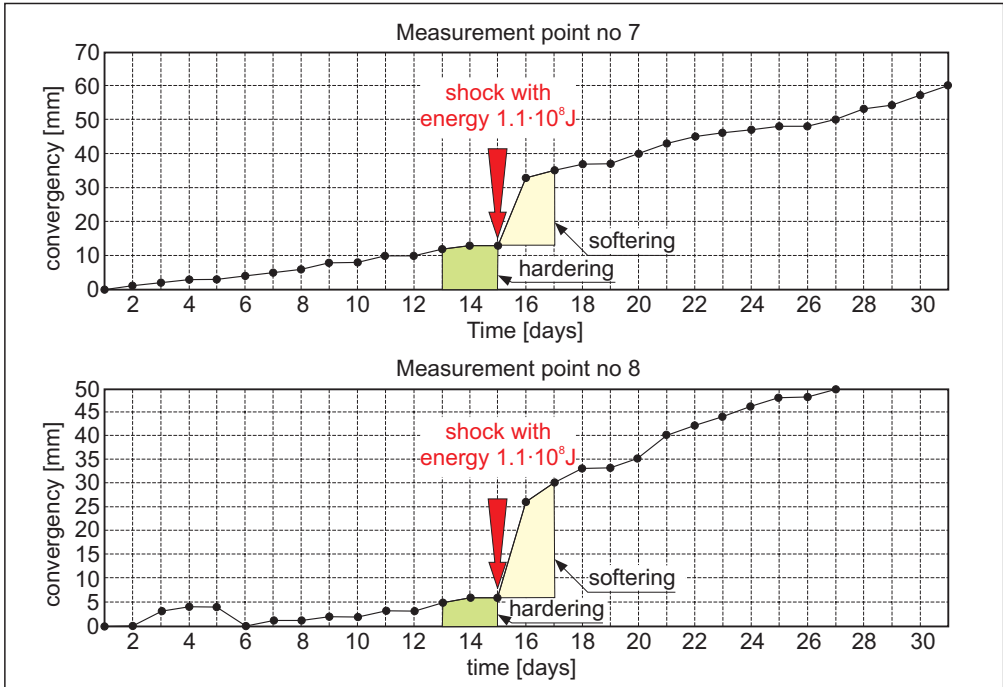


Fig. 3. The convergence of the roof layer before and after a shock which appeared on 15 August. 2007 with an energy level of  $1.1 \cdot 10^8$  J at two measured points in division 7/5 of the “Rudna” mine . The convergence before shock near 0 mm/day is the result of rock hardening and 20 mm/day is the result of softening

The most important element influencing the seismic moment and energy  $E$  of the seismic event can be written as:

$$E = -\mathcal{G}M\bar{\delta}/\mu \quad (11)$$

where:

- $\bar{\delta}$  — the average stress drops on the rupture and
- $\mathcal{G}$  — the efficiency of the seismic process.

It can be generally accepted that the energy of the seismic event is proportional to the  $\Sigma$ . The increase in stresses and the area of their intensive change due to an increase of width and depth of the fracture zone (possible a larger  $\Sigma$  when a larger depth of zone) cause an increase in energetic seismic events occurrence.

In summing up the considerations the following stages of the seismic generation process can be distinguished:

- Elastic bending gives a small, stable deflationary of roof seam,
- The ductile deformation turns into a ductile fracturing, redistribution of stresses and finally into splitting along horizontal borders and generation of seismic emission. Epicenters are located in the external parts of the bending beam (it's top or bottom),
- The horizontal extension of seismic fracturing is developed and the hypocenters are located along a local lineament,
- The coalescence of existing fractures and proceeds fracturing inwards into the roof seam gives seismic events with markedly higher energy,
- The new energetic events can coalescence and deeper fracturing gives very energetic seismic events,
- The bending resistance decreases gradually with an increase of the plastic area within the layer cross-section and the bending is faster. The breaking of the layer produces the largest seismic energy.

Mogi, 1963 divided earthquake sequences into three principal types: namely, main shocks, aftershocks, foreshocks-main shocks and earthquakes swarms. The mining shocks are assigned to the last category and the properties of those shocks can be analyzed according to the properties of this type of shock. In the paper (Helmstetter & Sorrento, 2002), the swarm category seismic events occurrence has been modelled. Let shock at time be  $t_i$  and with a position  $r_i$ . At a later time  $t = t_i + dt$  and position  $r = r_i + dr$  the seismic producing rate can be described using the formula:

$$\varphi_m(t - t_i, r - r_i) = q(m)\Theta(t - t_i)\psi(r - r_i) \quad (12)$$

where  $q(m)$  – gives the number of the seismic events with a magnitude  $m_i$  (logarithm energy of mining shocks) which is called energy distribution  $\Theta(t - t_i)$  – expresses the dependence of seismic activity in time (time distribution) and  $\psi(r - r_i)$  the spatial distribution.

All those elements are used for proving the proposed model.

#### 4. Stochastic scaling

A stochastic scaling (Koyama, 1997) gives the relationship between  $N_i(t)$ , the number of seismic events, within the  $i$ -th seismic magnitude range and  $N_{i+1}(t)$ , the number of seismic events, and in the  $i + 1$ -th seismic magnitude range. The  $N_i$  and  $N_{i+1}$  are random functions and statistically independent. The following relationship is defined as the stochastic scaling

$$\frac{a_d}{b_d} N_i(b_d t) \rightarrow N_{i+1}(t) \quad (13)$$

where  $a_d$  and  $b_d$  are scaling parameters and  $\rightarrow$  the stochastic convergence. Both scaling parameters are smaller than unity. When  $a_d = b_d$  the stochastic process is self-similar.

The scale invariant nature of function  $f(x)$  can be expressed by the function  $f(ax) = a^H f(x)$ , where  $H$  and  $a$  are positive constants.

For many seismic catalogues the Gutenberg-Richter law is valid:

$$\log(N_i(t)) = N\alpha - \beta \log(E_i) \quad (14)$$

The distribution of the frequency of events with energy  $m_i = \log(E_i)$  can be written as:

$$q(m_i) = K 10^{-\beta(m_i - m_0)} \quad (15)$$

for  $E_i$  greater than  $E_{\min}$   $K$  – constant  $m_0 = \log(E_{\min})$ .

Very often the parameters  $a_d$  and  $b_d$  are constant. For the model of generation discussed here parameters  $a_d$  and  $b_d$  should change, with the increase of fracture penetration inwards in the roof seam.

Stochastic scaling is also valid in describing the  $\Theta(t - t_i)$  function. The length of the critical gap between seismic events depends on the energy of the event and on the size of region representing data from the catalogue. If the probability density of events occurrence in time  $t$  has the form of the Poisson process:

$$P(\tau) = \lambda \exp(-\lambda\tau) \quad (16)$$

then a similar stochastic scaling can be introduced (Bak et al., 2002) as

$$\frac{a_d}{b_d} P_i(b_d t) \rightarrow P_{i+1}(t) \quad (17)$$

The cumulative number of seismic events in function of their energy has the fractal character (Consolini & Michels, 2002). Also the events waiting time depends fractally on the events energy. In result there is relationship between the frequency of events and the parameter  $\beta$ .

The frequency of events with energy greater then  $E_i$  ( $E_0$  minimum of energy in the catalog) and parameter  $\beta$  (Bak et al., 2002) can follow this relationship

$$\lambda_i(E_i/E_0)\beta L^{d_i} = \text{const} \quad (18)$$



where  $L$  may be estimated as the side of a square containing the area represented in the seismic catalogue, and  $d_i$  the parameter depending on the structure of data. Both elements in the stochastic scaling of mining seismic events and their frequency changes will be analyzed in a very active division of the copper deep mine in “Rudna”, in order to substantiate the relation between the seismicity of the region and the development of roof layer bending.

## 5. The “Rudna” mine

The data presented in the paper were recorded in the “Rudna” mine, Lower Silesia, Poland. The “Rudna” mine is exploited through deposits comprising three lithological rock zones with copper mineralization; namely: Rotliegendes sandstone, lower Zechstein shale and dolomites. The thickness of the ore seam varies from 0.5 to 20 m. Exploration is based on the room and pillar method with extra roof support, and partly with the elimination of cavities by rock or hydraulic backfilling and a controlled roof seam bending program. The ore has been excavated to the depth of 850-900 m.

The ore roof is built of beige or gray dolomite, and is very solid, but not homogenous, with stylonite joints, which can facilitate fracturing. Inside the ore there are also 3.5 cm diameter nets of anhydrite.

A seismological measuring system has been installed in the mine and seismological observations have been recorded continuously. On the basis of the recorded signals, the location of seismological event hypocenters and their energy are estimated. Seismological catalogues contain times of seismological event occurrences, the coordinates of event hypocenters and their energies. The catalogues consisting of the seismic events recorded in division 7/5 of the “Rudna” mine from 2005-2007 are subject of considerations in the paper.

There are many factors influencing the structure of mining seismic data. The most important are mining activity, the location of working faces and the ratio of exploited ore.

Also the geological structure and mechanical properties of rocks can decide the energy of seismic events. Empirical investigations of the mining seismicity generation are disturbed due to the blasting, provoking the seismic energy relaxation.

Two catalogues has been constructed for further analysis 2006 catalogue and 2007 catalogue. They should fulfill the following criteria:

- They consist of events with energy greater than  $10^5$  J. The appearance of such events must be prepared some time and they are less influenced by the local mining disturbances, which has shorter period of changes.
- The record of events with energy levels of  $10^8$  J should be included into catalogue near to its end. The changes of scaling parameters can be estimated on the basis of events relatively independent of the disturbances in mining activity.
- The events in each catalogue are inside the source area of the biggest final element. In the result it can be assumed, that there is a direct relation between the structure of the data and the strongest event occurrence.
- It should not be other energetic events with are not related to the roof bending which appeared during observations, which could markedly disturb the seismological generation process.

Only the 2006 catalogue fulfils these conditions. However catalogue 2007 is also similar to the catalog 2006 and is also analyzed.

There were three exploited mining fields “A”, “B” and “C” in division 5/7. The seismic emission is located along lineaments related to these fields. Field “C” is located near the “Biedrzychowa” fault, the main fault in this region. The diagrams shown in fig. 4 present the distribution of energy shocks in both catalogues. The number of strong shocks in this division is larger than in the average division of the “Rudna” mine. Many strong shocks with energy greater than  $10^5$  J were induced by blasting (60% in 2006, 40% in 2007 year): a method preventing the unexpected seismic energy relaxation. All of the events would be related to the roof layer bending except event  $10^8$  J in 2007, which was the result of activating the regional fault known as “Biedrzychowa”.

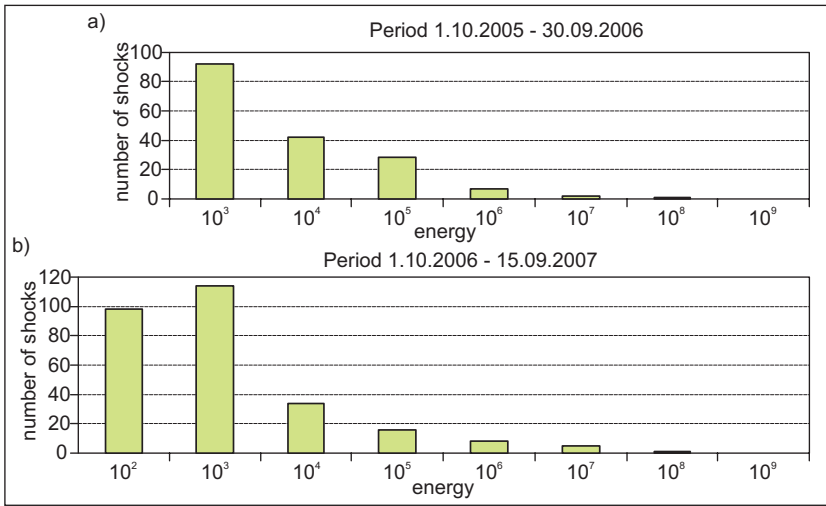


Fig. 4. The distribution of seismic energy during exploitation of division 7/5, “Rudna” mine (a) in the period 01.10.2005-30.09.2006 and (b) in the period 01.10.2006-15.09.2007

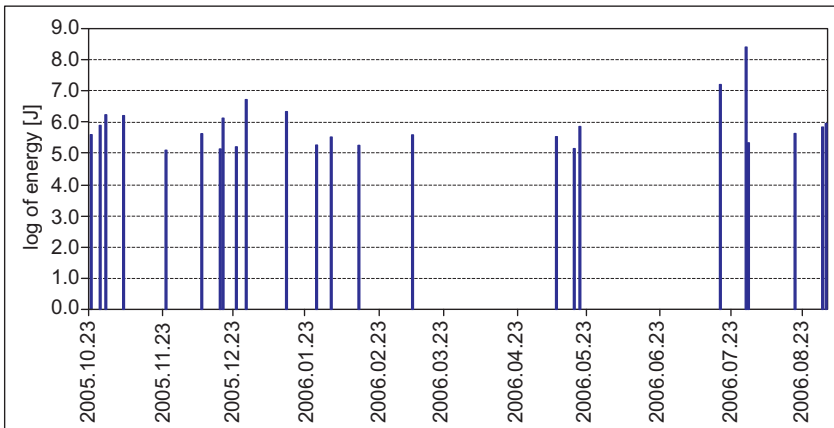


Fig. 5. The time distribution of seismic events which occurred in division 7/5 of the “Rudna” mine in the period 01.10.2005-30.09.2006. Data greater then  $10^5$  J

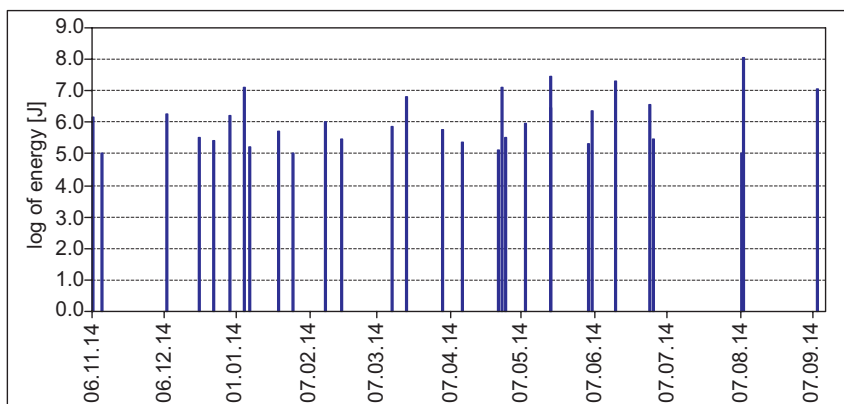


Fig. 6. The time distribution of seismic events which occurred in division 7/5 of the "Rudna" mine in the period 01.10.2006-15.09.2007. Data greater than  $10^5$  J

## 5.1. The spatial distribution

One of the consequences of the proposed model of seismic events generation is linear distribution of the seismic epicenters. As it has been shown the maximum of normal stresses runs along the maximum bending curvature line.

The position of epicenters from the 2006 catalogue is shown in fig 7. Two lineaments were distinguished, one along the block "A" and the second along block "B".

The events related to block "B" were analyzed statistically. It seems that the straight line fits perfectly the positions of epicenter locations, as shown on fig. 8. The correlation coefficient between empirical and fitted data is equal to 0.97 and the standard deviation is equal to 38 m, when the length of line is almost 800 m. The lineament along block "A" seems to be similar. The errors can be related to accuracy of the estimation and changes of epicenters positions due to the depth of the hypocenters.

The frequency of the shocks in which the distance between the following events is up to 200 m or up to a multiplication of this distance, is shown in fig. 9. The result can be interpreted as the development of seismicity in the "nest" within a 200 m distance.

The distance between the following shocks chosen from the 2006 catalogue and the final shock with energy of  $2.3 \cdot 10^8$  J is shown in fig. 10. The distance of 700 m is less than the length of source area for the final shock. It means that the fractures developed before a strong final shock from one side are creating the conditions for the final strong seismic relaxation (through the hierarchic breaking along the lineament as has already been suggested in this paper), but from the other side are activated in the final fracturing.

The same presentations for the 2007 catalog (Fig. 11 and Fig. 12) shows the difference in its structure in a comparison with the 2006 catalogue.

The problem with inhomogeneity of the data from this catalogue is obvious. The strongest shock with energy over  $10^8$  J isn't located along the lineaments but aside (along the regional fault "Biedzychowa"). However, most of the epicenters, being similar to those in the catalogue

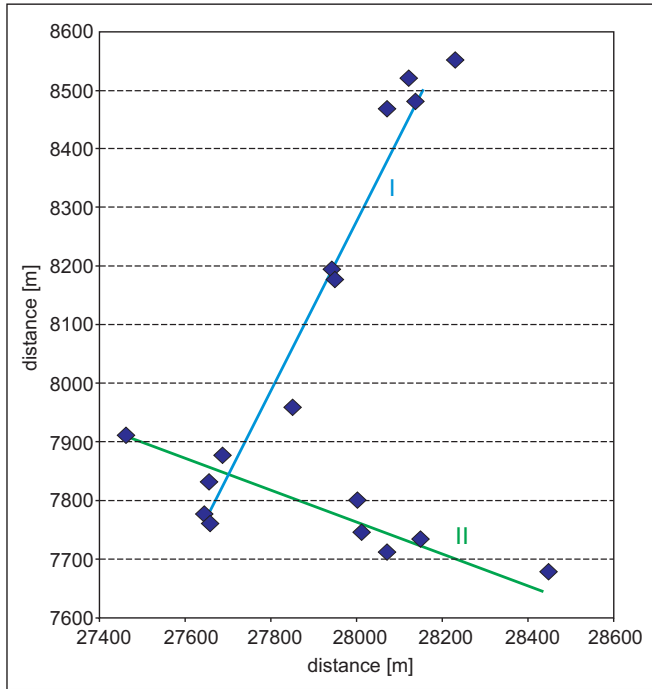


Fig. 7. The distribution of the epicenters from the 2006 catalogue. Data registered in division 7/5 of the “Rudna” mine in the period 01.10.2005-30.09.2006. Data greater than  $10^5$  J

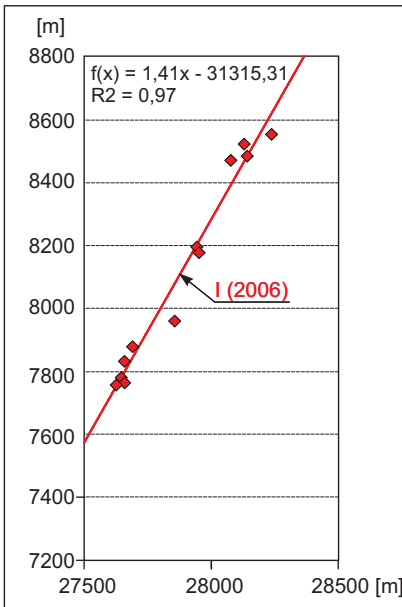


Fig. 8. The position of one of seismic data lineaments along the “B” front. Events with energy greater than  $10^5$  J recorded from February to November 2006. Seismic events, which occurred in division 7/5 of the “Rudna” mine

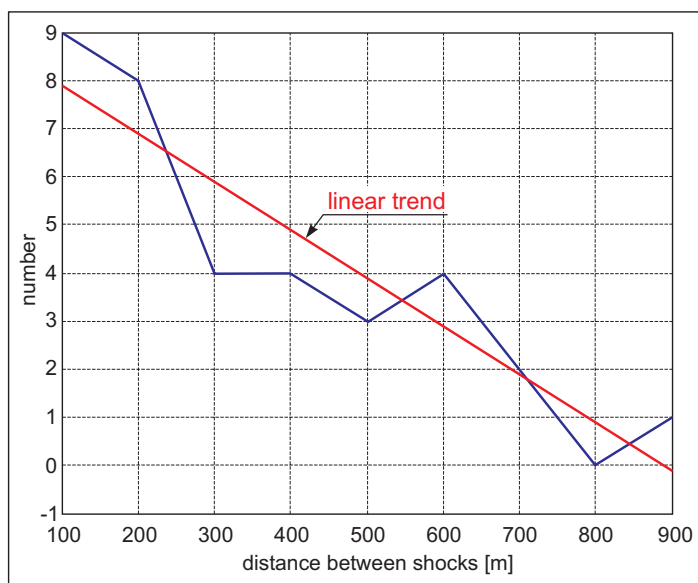


Fig. 9. The relation between the frequency of events as a function of the distance between the following events. Events with energy greater than  $10^5$  J recorded from February to November 2006. Seismic events, which occurred in division 7/5 of the “Rudna” mine

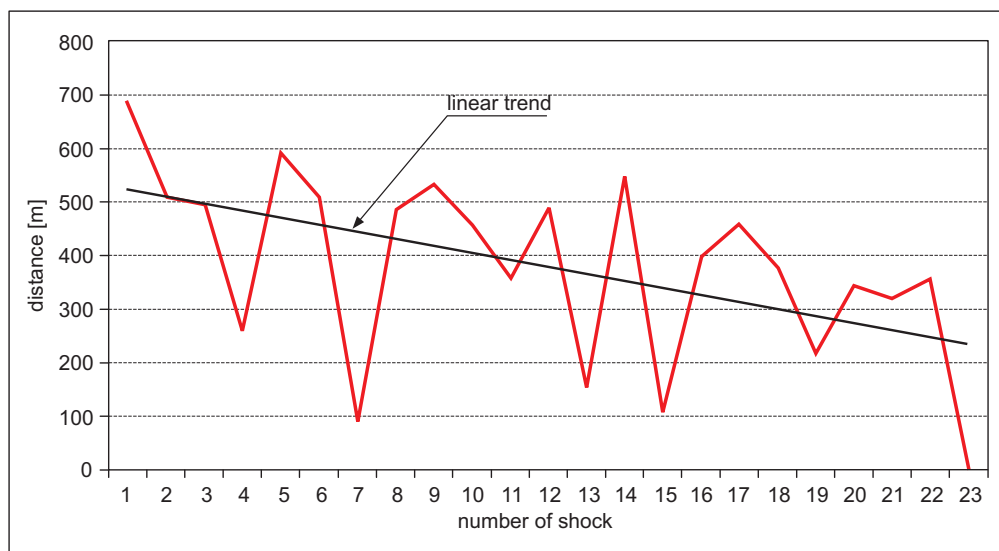


Fig. 10. The distance between the epicenter of the strongest shock with energy at  $2.3 \cdot 10^8$  J and the epicenters of the following shocks from the 2006 catalogue. Events with energy greater than  $10^5$  J recorded from February to November 2006. Seismic events, which occurred in division 7/5 of the “Rudna” mine

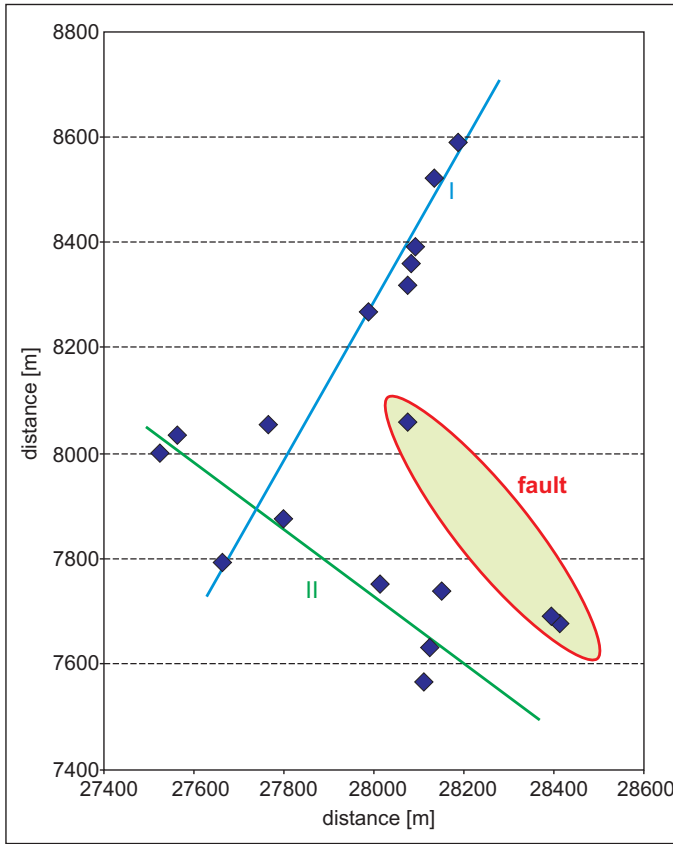


Fig. 11. The distribution of the epicenters for the data from the 2007 catalogue. Seismic events, which occurred in division 7/5 of the “Rudna” mine in the period 01.10.2006-15.09.2007. Data greater then  $10^5$  J

of 2006, fits to two lines. In result the similar analyzes has been preceded for catalogue 2007 as for catalogue 2006 in spite of mensioned above disturbances.

The distribution of the distances of subsequent shocks from a strong shock with energy  $2 \cdot 10^7$  J which occurred near to the end of the catalogue is shown in fig. 16. Similarly to results shown in fig. 14 the shocks are more close to the strong event epicenter with increasing time.

### 5.2. Energy distribution

As was shown, the seismic data can be divided into  $m$  groups depending on their energy and the frequency in the group is described by the formula (15): The expected value of  $m$  can be calculated as

$$E(m) = \int_{m_o}^{m_{\max}} m q(m) dm \tag{19}$$

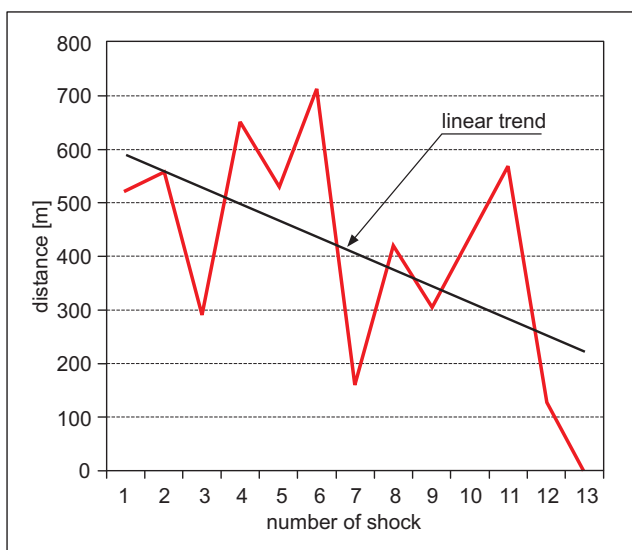


Fig. 12. The distance between the epicenter of the strongest shock with an energy level of  $2 \cdot 10^7$  J and the epicenters of the following shocks from the 2007 catalogue. Seismic events, which occurred in division 7/5 of the “Rudna” mine in the period 01.10.2006-15.09.2007. Data greater than  $10^5$  J

After calculations

$$E(m) = K \left( \left( \frac{1}{(\log(10))^2 \beta^2} + \frac{m_0}{\log(10)\beta} \right) - \left( 10^{-\beta(m_{\max} - m_0)} \left( \frac{m_{\max} \beta \log(10) + 1}{(\beta(\log(10))^2)} \right) \right) \right) \quad (20)$$

This formula gives information related to the model of seismic events generation. If the generation process is stationary and parameters “a” and “b” of stochastic scaling are constant, then  $E(m)$  shouldn’t depend on time. On the contrary, if the bending process generate seismic events as was mentioned before, the parameters of stochastic scaling have to change in time and as a result  $E(m)$  should also increase (particularly  $m_{\max}$  should increase in time).

The average energy from 8 subsequent shocks has been calculated from both catalogs and the results are shown in fig. 13 (catalogue 2006) and fig. 15 (catalogue 2007). The presentation of results starts from the 8-th shock. The increase of energy before strong seismic events which occurred at the end of the presented set of seismic records is evident here. This result strengthens the relevance of the proposed generation model.

### 5.3. Time distribution

The next expected indicator of the relation between bending of the roof layer and seismicity is the change in waiting time (time between subsequent shocks). As was discussed before, the changes in this parameter should indicate the dependence of the stochastic scaling parameters on time in result of the roof layer bending.

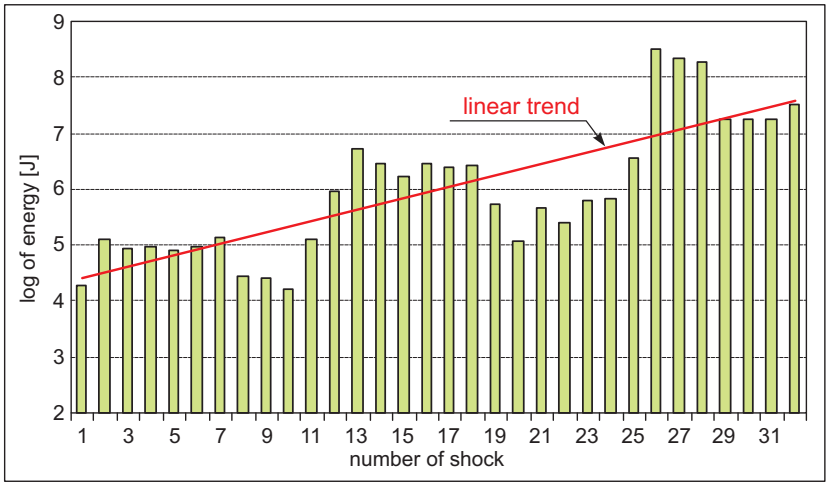


Fig. 13. The average logarithm of seismic energy for 8 subsequent seismic events with energy greater than  $10^5$  J, recorded from 15 October 2005 to 1 August 2006. Seismic events, which occurred in division 7/5 of the “Rudna” mine

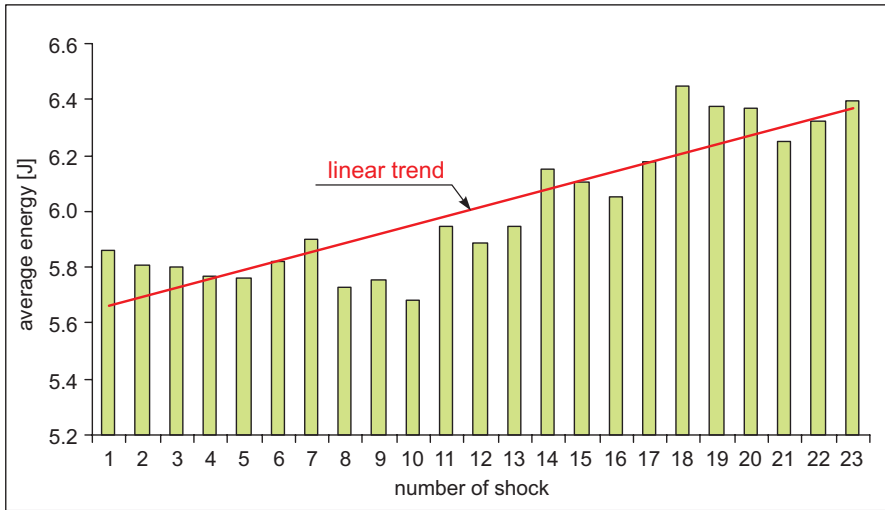


Fig. 14. The average logarithm of seismic energy for 8 subsequent seismic events with energy greater than  $10^5$  J, recorded from 6 November 2006 to 11 June 2007. Seismic events, which occurred in division 7/5 of the “Rudna” mine

Those values depend more intensively on the strategy of mining works. However result of calculations confirms the expected behavior based on the proposed seismic generation model.

The time at which 8 subsequent seismic events occurred was calculated for both catalogues: 2006 (for energy greater than  $10^4$  J) and 2007 (for energy greater than  $10^5$  J). The results are



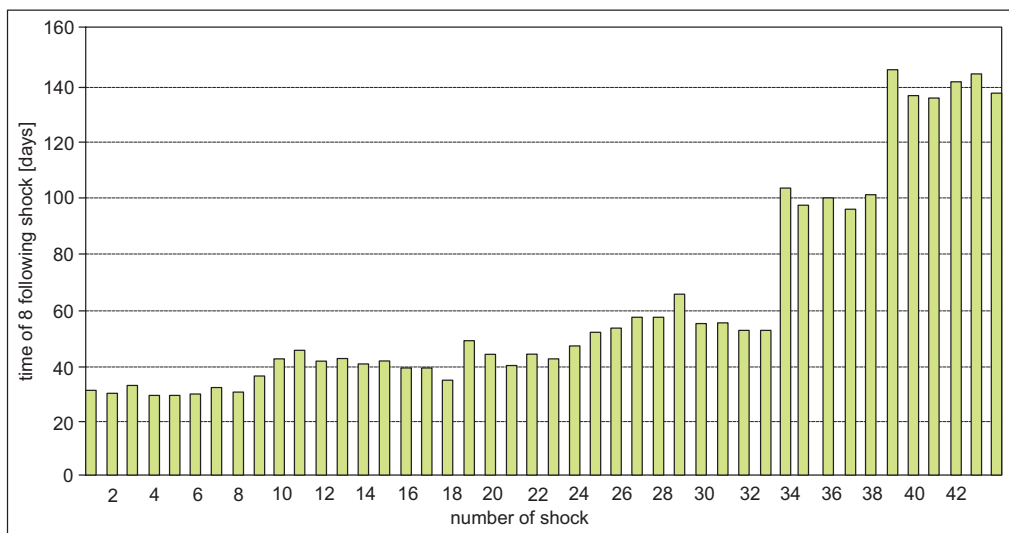


Fig. 15. The sequence of the shocks from 2006 catalogue. The time at which the 8 subsequent shocks occurred with energy greater than  $10^4$  J in function of the following shocks number in dependence of the number of the shocks recorded in the catalogue. Registrations from 7.10.2005 to 31.08.2006. Seismic events, which occurred in division 7/5 of the “Rudna” mine

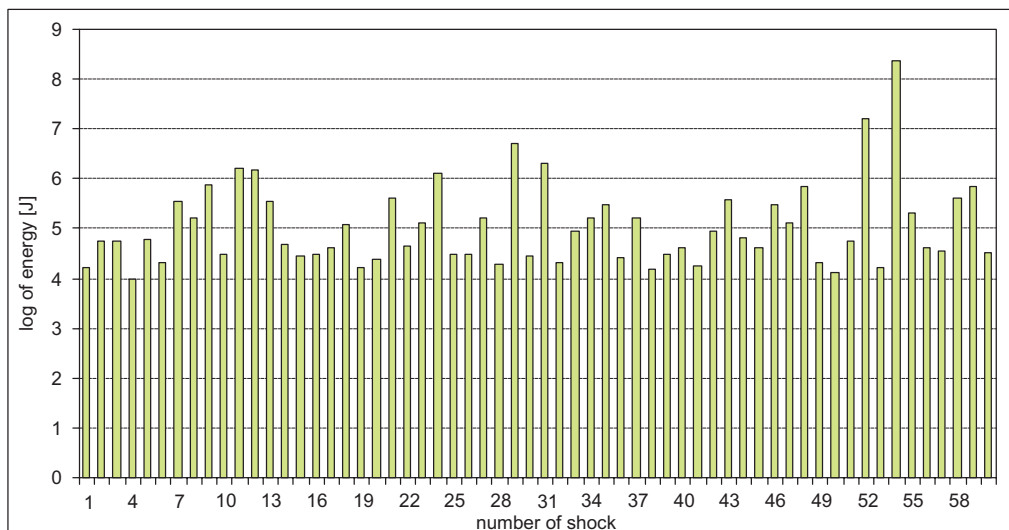


Fig. 16. The logarithm of seismic events distribution (energy greater than  $10^4$  J). Registrations from 7.10.2005 to 31.08.2006. Seismic events, which occurred in division 7/5 of the “Rudna” mine

shown in fig. 15 and fig. 17. Similarly, as in the case of energy distribution, the frequency of seismic data isn't stationary.

The decrease of average frequency of seismic data before the strong seismic events which appeared in August 2006 (shown in fig. 16), has an exponential character. Frequency calculated from the 2007 catalogue shown in fig. 17 has two maxima, both before very strong seismic events while the average logarithm of energy has only one maximum. If the average frequency is calculated from 16 subsequent records there is only one maximum.

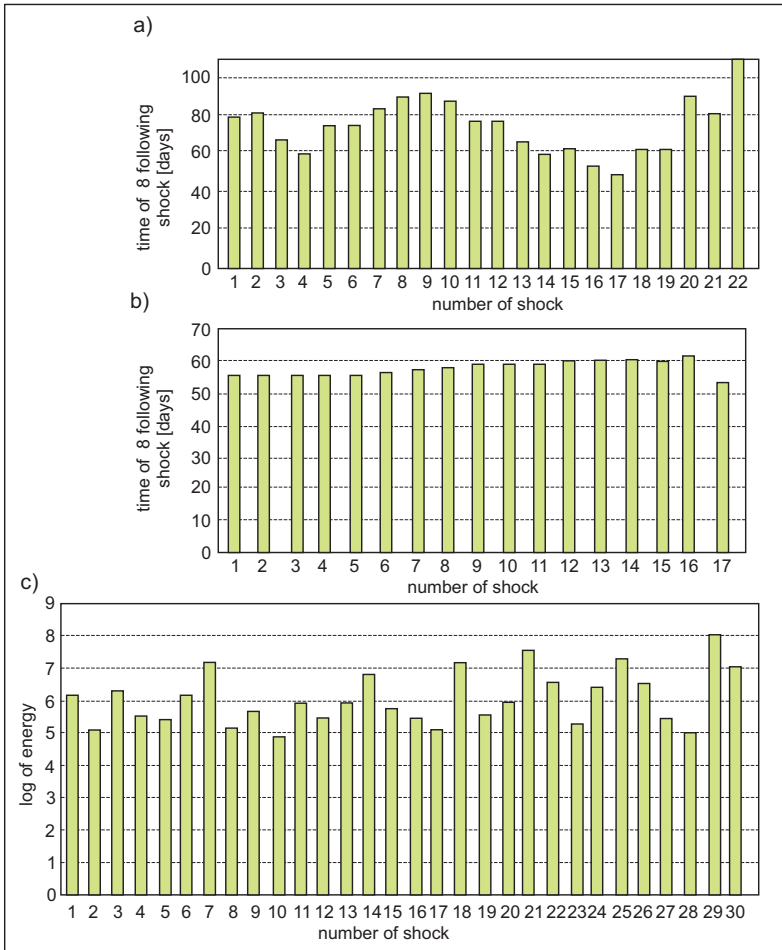


Fig. 17. The sequence of the shocks from 2007 catalogue, (a) The time at which the 8 subsequent shocks occurred as a function of the following shocks number (b) The time at which the 16 subsequent shocks occurred (divided by 2), both with energy greater the  $10^5$  J in function of the following shocks number (c) The logarithm of seismic events distribution (energy greater than  $10^3$  J).

Registrations from 01.10.2006 to 15.09.2007. Seismic events, which occurred in division 7/5 of the “Rudna” mine

## 6. The dynamic model of average mining shocks energy

The number of seismic events in the catalogues 2006 and 2007 with energy greater than  $10^5$  J, represents only about 20% of the total number of events with energy greater than  $10^3$  J. But the weak shocks are the result of local, temporary conditions and their epicenters are scattered much wider than the epicenters of the strong shocks. The procedures for processing such data having the structure of earthquake swarm can be based on the dynamic model. The general dynamical model used to describe the temporal variation of the swarm earthquakes was proposed by Ouchi (Ouchi, 1992). It has form

$$\frac{dn(t)}{dt} = F(n, c_1, c_2, \dots, c_n) \quad (21)$$

where  $n(t)$  denotes the number of earthquakes,  $t$  time  $c_i$  various parameters as stresses, structure of rocks and other properties of medium.

In this paper this formula has been used for dealing with average seismic energy not the number of events

The changes in the average seismic energy of mining shocks can also be treated as a parameter in dynamic system. This system is described by the relation

$$\frac{dE(t)}{dt} = F(n, c_1, c_2, \dots, c_n) \quad (22)$$

where  $E$  – average energy calculated from following events taken from the total catalogue (energy over  $10^3$  J).

The  $F$  function is proposed in the form:

$$F(\log_{10}(E)) = s + \log_{10}(E(\alpha_0 - \beta_0 E)) \quad (23)$$

where  $\alpha_0$  describes the production rate of energy and  $\beta_0$  the reduction rate,  $s$  – the parameter depending on the level of seismic activity.

The average of 8 subsequent seismic events energy calculated from the total catalogue provides information from the shorter period (different scale level). The result of the calculations is shown in fig. 18 (for the 2006 catalogue) and fig. 19 (for the 2007 catalogue). The dynamic model shown in fig. 20, fits to two periods preceding the emission of strong shocks for data calculated from the 2006 catalogue and one for data calculated from the 2007 catalogue (both catalogues contain seismic events with energy greater then  $10^3$  J).

The fitting model has the following parameters  $\alpha_0 = 1,4$ ,  $\beta_0 = 0,01$  (Fig. 20). The seismic shock with energy greater than  $10^8$  J, which was registered in 14.08.2007, is not preceded by the model. This shock, as was mentioned, isn't the result of roof layer bending but reactivation of the existing fault. It can be concluded that the proposed dynamic model is sensitive on the changes of scaling parameters result of the bending model.

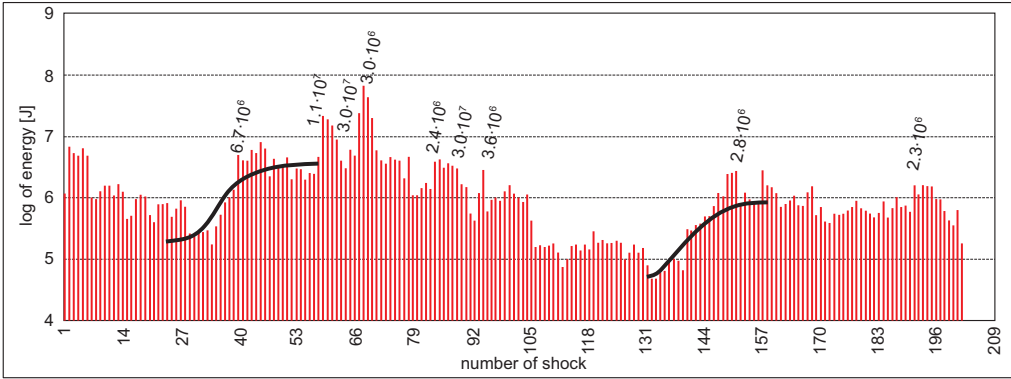


Fig. 18. The distribution of average seismic energy calculated from 8 subsequent data taken from the total catalogue (registration from 7.10.2005 to 31.08. 2006 ) of seismic records greater than  $10^3$  J. Fitting Seismic events, (black lines represent the dynamic model shown in fig. 20), which occurred in division 7/5 of the “Rudna” mine

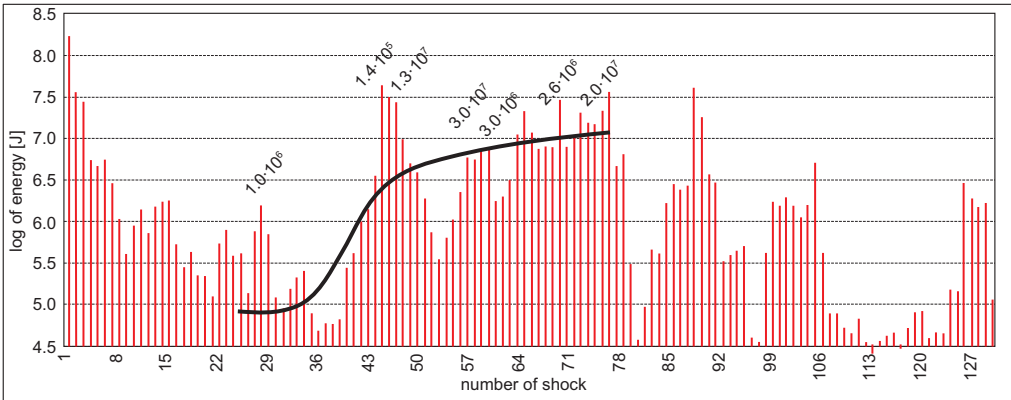


Fig. 19. The distribution of average seismic energy calculated from the data of 8 subsequent shocks taken from the 2007 catalogue (registration from 01.10.2006 to 15.09.2007), of seismic records greater than  $10^3$  J. Seismic events, (black line represents the dynamic model shown in fig. 20), which occurred in division 7/5 of the “Rudna” mine

## 7. Conclusions

There is lot of obstacles in recognizing the dynamic processes which lead to an earthquake. One of them is the large distance from the registration devices and the source of earthquakes. In the case of mining seismic events, the distance is small and the stress-strain system which is in the rock mass prone to seismic emissions can be approximated on the basis of empirical observations.

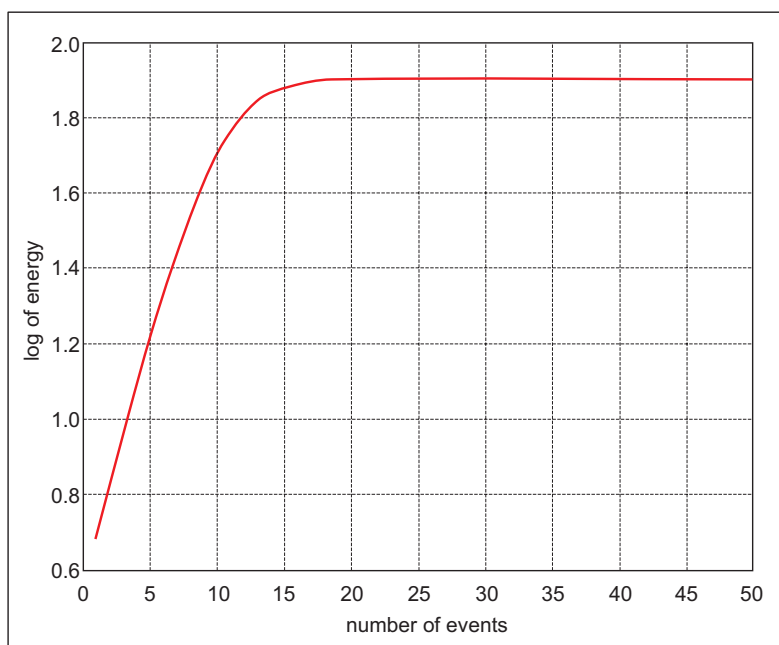


Fig. 20. The dynamic model fitted to changes of average seismic energy calculated from 8 data events, greater than  $10^3$  J

The stresses of the bending roof layer are assumed in many Polish underground mines to be the source of rock-burst risk. These stresses develop over time and it is shown in the paper that the average energy of seismic events and their frequency are developing in accordance with it. The energy release is preceded by the increase in average energy calculated in the short based data. The increase can be described by the dynamic model.

The distribution of stresses, average energy of seismic events and their frequencies can be described by the stochastic processes. Significant trends in these processes can be explained by the bending of the roof layers over the exploited area.

There is also additional information available such as the convergence measurements, the splitting of roof layer observations and the measurements of roof deformations. This information, together with seismic data, can be successfully interpreted on the basis of the bending model of the roof layer.

### Acknowledgments

The Ministry of Science and Higher Education supported the work within the framework of the research project no N52393539.

## References

- Bak P., Christensen K., Danon L., Scanlon T., 2002. *Unifield scaling law for earthquakes*. Phys Rev Let 88: 178501.
- Borešić A.P., Schmidt R.J., Sidebottom O.M., 1993. *Advanced mechanics of materials*. John Wiley and Sons, New York.
- Consolini G., Michelis P., 2002. Fractal time statistics of AE-index burst waiting times: evidence of metastability Non-linear Processes in Geophysics nr 9, 419-423.
- Dubiński J., 1999. *Concentration of coal exploitation and mining hazard Central Mining Institute*. Katowice 219 p. (in polish).
- Dubiński J., Konopko W., 2000. *Rock-burst estimation, forecast, prevention Central Mining Institute*. Katowice 378 p. (in polish).
- Helmstetter A., Sorento D., 2002. *Diffusion of epicenters of earthquake aftershocks, Omori law, and generalized continuous-time random walk models*. Physical Review E 061104 (23 p.).
- Koyama J., 1997. *The complex faulting process of earthquakes*. Kluwer Academic Publishers 195 p.
- Lasocki S., 2005. *Probabilistic analysis of seismic hazard posed by mining-induced events*. Proceedings of the 6th Int. Symp. on Rockbursts and Seismicity in Mines Controlling on Seismic Risk ACG, Perth, 151-156, eds Potvin Y. & Hudyma M., Australian Centre for Geomechanics, Nedlands, Western Australia.
- Lasocki S., 2008. *Some unique statistical properties of the seismic process in mines*. in Proceedings of the 1st Southern Hemisphere International Rock Mechanics Symp., Vol. 1: Mining and Civil, Perth, 667-678, ed. ed. Potvin Y., Australian Centre for Geomechanics, Nedlands, Western Australia.
- Marcak H., 2002. *The influence of strata and tectonics on the rockburst risk in polish mines In Seismogenic Process Monitoring*, Ogasawara H., Yanagidani T., Ando M., eds, Balkema, 51-63.
- Marcak H., 2011a. The seismic activity due to the bending of exploited seam roof. Proceedings of 22<sup>nd</sup> World Mining Congress 11-16 September Istanbul
- Marcak H., 2011b. *Influence of inelastic deformations in bending roof layers on the seismicity in the underground mines Materials and Works of GIG*. Proceedings of the Conference "Tapania 2011" Kocierz (in polish).
- Mogi K., 1963. *Some discussion on aftershocks, foreshocks and earthquakes swarms. The fracture of a semi finite body caused by an inner stress origin and its relation to the earthquake phenomena*. Bull. Earthq. Res. Inst. Tokyo Univ 41, 615-658.
- Orlecka-Sikora B., 2010. *The role of static stress transfer in mining induced seismic events occurrence, a case study of the Rudna mine in the Legnica-Glogow Copper District in Poland Geophys. J. Int.* 182, 1087-1095.
- Ouchi T., 1993. *Population dynamics of earthquakes and mathematical modeling*. PAGEOPH, 140, 15-28.
- Rice J.R., 1980. *The mechanics of earthquake rupture in Physics of the Earth Interior*. (Proceedings of International School of Physics "Enrico Fermi" Italian Physical Society North-Holland Pub. Co, 515-649.
- Rice J.R., Ruina A.L.. 1983. *Stability of steady frictional slipping*. Trans. ASME, J. Appl. Mech. 50, 343-349
- Saustowicz A., 1955. *Rock-mass mechanics*. Wydawnictwo Górniczo-Hutnicze Katowice.
- Węglarczyk S., Lasocki S., 2009. Studies of Short and Long Memory in Mining-Induced Seismic Processes Acta Geophysica Special Section: Triggered and Induced Seismicity Vol. 57, No. 3, 696-71

Received: 29 November 2011